Mathematical Biosciences and Engineering, 16 (4): 1750–1760.
DOI: 10.3934/mbe.2019084
Received: 27 December 2018
Accepted: 12 February 2019
Published: 06 March 2019

http://www.aimspress.com/journal/MBE

Research article

Comparison of airflow characteristics after Draf Ⅲ frontal sinus surgery and normal person by numerical simulation

Cheng Li[1], Xiuzhen Sun[2], Ming Zhao[3], Shen Yu[3], Qian Huang[1], Xiaoqing Zhang[1], Zhenxiao Huang[1], Shunjiu Cui[1] and Bing Zhou[1,*]

[1] Department of Otolaryngology-Head and Neck Surgery, Beijing Tongren Hospital, Capital Medical University, Beijing, China
[2] Department of Otolaryngology-Head and Neck Surgery, Second Affiliated Hospital of Dalian Medical University, Dalian, China
[3] Department of Engineering Mechanics, Dalian University of Technology, Dalian, China

* **Correspondence:** Email: entzhou@263.net.

Abstract: Draf III frontal sinus surgery is confirmed as an effective surgical treatment for refractory sinusitis and frontal sinus tumors, etc. Although it has been reported to improve symptoms and reduce the recurrence rate of polyps significantly, the study of airflow characteristics in frontal sinus after Draf III is still rare, especially compared with normal person. This study was designed to describe the airflow characteristics of frontal sinus after Draf III procedure and differences compared with normal subject. One patient with refractory sinusitis received Draf III procedure15 months ago, and one normal person were selected retrospectively. The two subjects reported no discomfort and no abnormalities in their paranasal sinus within computed tomography scans. Computational fluid dynamics and numerical simulation calculation was performed with the finite volume method. The quantitative indexes of airflow in the frontal sinus of Draf III and normal subjects were achieved. Areas of relatively high-pressure and high wall shear stress located in a posterior part of frontal sinus ostium in both models. Inside frontal sinus, pressure and velocity of flow between Draf III and normal models were statistically significant differences ($p < 0.01$) after analyzed by Mann-Whitney U test. But airflow pattern of each section in frontal sinus was basically the same. Draf III sinus surgery is able to achieve nasal airflow patterns similar to those of normal person. Although values of airflow pressure and velocity were different from normal person, patients could have no subjective discomfort after surgery. “Frontal T” structure is a key anatomical site interacted with airflow to be an important cause of postoperative edema after Draf III procedure.

Keywords: Draf III; modified Lothrop procedure; numerical simulation; computational fluid dynamics; airflow

1. Introduction

Draf III frontal sinus surgery is also known as the modified Lothrop procedure. Unlike conventional endoscopic frontal sinus surgery, Draf III procedure removes front end of bilateral middle turbinate, corresponding nasal septum part, frontal processes of the maxilla and frontal nasal crest. Part of frontal sinus septum is also removed. An enlarged midline frontal sinus drainage channel is formed for bilateral frontal sinus fusion [1,2]. Scope of Draf III procedure is more extensive, especially surrounding the frontal sinus, than functional endoscopic surgery (FESS) which used to be the most common type of endoscopic surgery. This radical procedure can extendedly remove inflammatory-loaded mucosa and hyperplastic bone in order to form spacious frontal sinus ventilation with drainage channel. It is widely used in the surgical treatment of recurrent chronic sinusitis and nasal polyps, especially refractory sinusitis, frontal sinus mucus cysts, and frontal sinus tumors [3,4]. In the treatment of chronic recurrent sinusitis, especially patients with asthma, the choice of nasalization combined with Draf III procedure can significantly reduce surgical failure and improve the surgical outcomes [5–9]. Additionally, combined with medical therapy, recurrence of nasal polyps after radical surgery based on ethmoid sinus and frontal sinus can effectively reduce [10,11]. Although better surgical outcomes can be obtained by reducing inflammatory load, postoperative nasal structure is very different from that of a normal person for radical and extensively resection range.

It remains unknown, whether nasal sinus airflow after this radical resection can recover to normal physiological respiratory airflow characteristics. Computational fluid dynamics (CFD) is a common method to study the airflow characteristics and had been widely used in various fields of medicine [12–14]. Our previous study showed that postoperative nasal discomfort is not associated with the surgically expanded volume, nasal resistance, or total postoperative nasal volume after the correlation analysis [9]. Computational fluid dynamics study showed that expansion of the windowing at the posterior end of nasal septum does not affect nasal airflow patterns [15]. However, there was no exploration of airflow characteristics in frontal sinus in the previous study. In this study, we used computational fluid dynamics and numerical simulation of real cases to describe the airflow characteristics of the frontal sinus after Draf III procedure and compared the findings with the normal person to explore the effects of surgery on nasal airflow.

2. Materials and method

2.1. Study design and patient data

We retrospectively selected one patient with refractory sinusitis received Draf III procedure 15 months ago and one normal subject. All paranasal sinus computed tomography (CT) scans showed no abnormal mucosal thickening (Lund-Mackay score of 0). Lund–Kennedy score of postoperative nasal endoscopic local mucosa was also 0 point except for scar. The patient reported no discomfort.

2.2. Three-dimensional CT reconstruction

A 256-row high-resolution spiral nasal sinus CT scanner was used (resolution, 512 × 512; layer thickness, 0.67 mm; window width, 2000 HU; window position, 200 HU). A DICOM format file was used for three-dimensional reconstruction with Mimics 17.0 software (Materialise NV, Leuven, Belgium).

2.3. Boundary conditions and parameter settings

Models were meshed by Ansys 15.0 software (Ansys, Canonsburg, PA, USA). 1,663,773 meshes of Draf III and 1,597,684 meshes of normal model were selected as the appropriate grid number model after mesh independence test.

The density of gas defaulted to an air density of 1.225 kg/m^3. Viscosity of gas was the default value of 1.7894 × 10^{-5} kg/(m s), that is, simulating airflow field at temperature of 287.37 K. The steady-state and k-ε turbulent modes were used to calculate parameters. Plane of bilateral front anterior nares was selected as the inlet plane with 1 standard atmosphere setting as inlet pressure. Outlet plane was settled at nasopharynx with pressure of default value (0 Pa). Inspiratory phase was simulated.

2.4. Definition of drainage plane of frontal sinus after Draf III procedure

A plane parallel to the x-y plane was made through the long (posterior border of perpendicular ethmoid lamina resection) and short crus (posterior margins of frontal sinus floor resection) junction point of "Frontal T" structure which was defined by Draf [16]. The section of this plane was defined as drainage plane of frontal sinus after Draf III procedure.

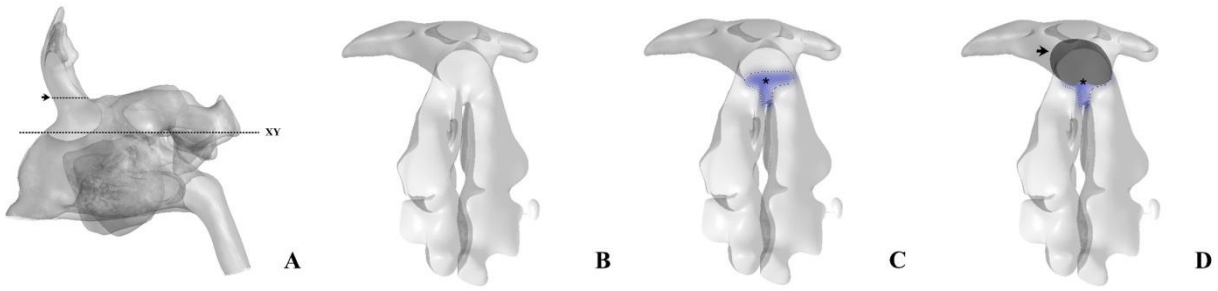

Figure 1. The step of drainage plane positioning of frontal sinus after Draf III procedure. A: Left side view of Draf III model with x-y plane labeled as "xy". Drainage plane of frontal sinus (→) was parallel to the x-y plane. B: Bottom view after cutting the model horizontally at x-y plane. C: "Frontal T" structure (Blue part). Long and short crus junction point (*). D: Drainage plane of the frontal sinus (dark shaded).

2.5. Selection of cross-section of intra-frontal sinus

The vertical distance between frontal sinus ostium and the highest point of frontal sinus vertex

was equally divided into 100 sections and then numbered, with frontal sinus ostium plane as 1 and frontal sinus vertex as 101. Values of pressure and velocity in all 100 sections were obtained by Ansys 15.0. Four sections (Nos. 1, 25, 50, and 75) were selected to compare the similarities and differences of airflow patterns between the two models.

2.6. Statistical analysis

SPSS 22.0 was used for analysis in this study, Mann-Whitney U test was used and $p < 0.05$ was considered statistically significant.

3. Results

3.1. Airflow characteristics of frontal sinus ostium

Average airflow pressure in frontal sinus ostium after Draf III procedure was 0.71×10^5 Pa. Relative pressure difference (maximum pressure - minimum one) was 0.11×10^5 Pa. Average airflow velocity was 39.32 m/s. Airflow pressure reduced by 30.1% compared with inlet plane. Average pressure of normal model was 0.89×10^5 Pa. Relative pressure difference was 72.5 Pa. Average airflow velocity was 3.56 m/s.

Cloud map showed that pressure distribution of frontal sinus ostium after Draf III procedure was similar to normal model (Figures 2-A1, A2). A relatively high-velocity area (Figure 2-B1) was present in Draf III model at the posterior portion of frontal sinus ostium compared with the normal model (Figure 2-B2). Streamline diagram (Figures 2-C1, C2) showed vortex formation in frontal sinus ostium of both models. There is a relatively high-pressure area at the posterior part of frontal sinus in both models with pressure gradually increased from center to periphery of the frontal sinus ostium (Figure 2-D1, D2).

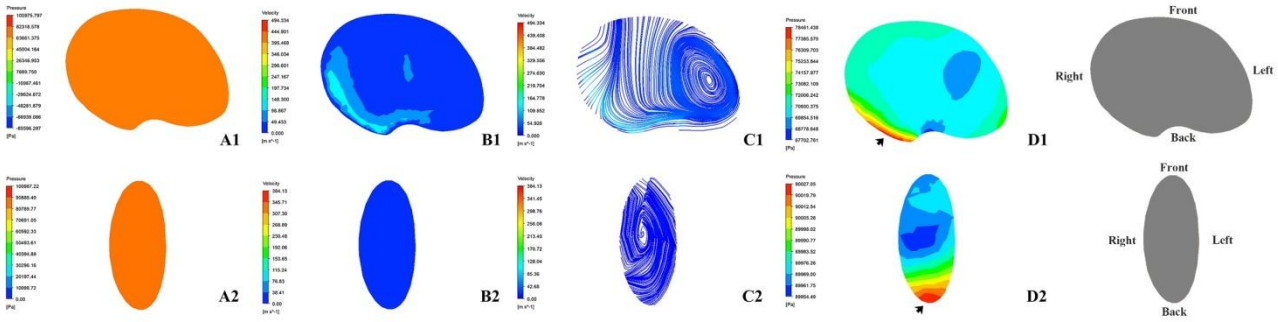

Figure 2. Airflow characteristic patterns in the plane of frontal sinus ostium. A1/A2: Pressure field of Draf III model/normal model (global pattern). B1/B2: Velocity field of Draf III model/normal model (global pattern). C1/C2: Streamline of Draf III model/normal model (global pattern). D1/D2: Pressure field of Draf III model/normal model (local pattern). Maximum pressure (→). (Global pattern: scale range of cloud map includes outcomes of the entire nasal model. Local pattern: scale range of cloud map just includes outcomes of the current plane.)

3.2. Airflow characteristics of intra-frontal sinus

Average pressure was 0.71 × 10^5 Pa inside the frontal sinus after Draf III procedure, with relative pressure difference of 0.11 × 10^5 Pa. Average velocity was 28.6218 m/s. Additionally, the maximum wall shear stress was 96.99 Pa with an average value of 12.53 Pa. High wall shear stress area mainly appeared around the frontal sinus ostium (Figure 3N). After frontal sinus extracted separately, the highest wall shear stress was located on the right lateral wall of frontal sinus ostium (Figure 3n).

In normal model, average pressure was 0.88 × 10^5 Pa (19.3% higher than that in Draf III model), with relative pressure difference of 0.19 × 10^5 Pa. Additionally, average velocity was 1.22 m/s. The maximum wall shear stress was 67.5301 Pa with average value of 0.34 Pa. The wall shear stress of frontal sinus was lower than that of the whole nasal cavity (Figure 3M). The highest wall shear stress was located on the posterior lateral wall of frontal sinus ostium (Figure 3m).

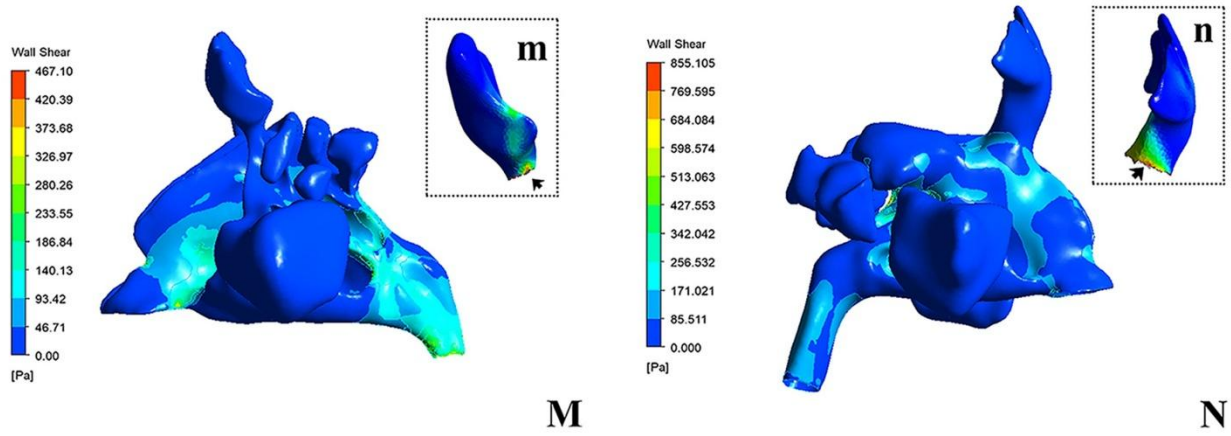

Figure 3. Wall shear stress compared with Draf III and normal models. M/N: Distribution of wall shear stress in normal model/Draf III model (global pattern). m/n: Distribution of wall shear stress in frontal sinus of normal model/ Draf III model (local pattern). Maximum wall shear area (→).

By using Mann-Whitney U test, statistically significant differences were shown of pressure and velocity between Draf III and normal models (Pressure: $p < 0.01$; Velocity: $p < 0.01$). Distribution diagram (Figure 4) showed lower pressure, higher velocity and change amplitude of velocity in Draf III model than in normal subject. But streamline diagram (Figures 5-G1, G2) showed similar airflow patterns in the same cross-section of frontal sinus between Draf III and normal models, with one or more airflow vortexes formed.

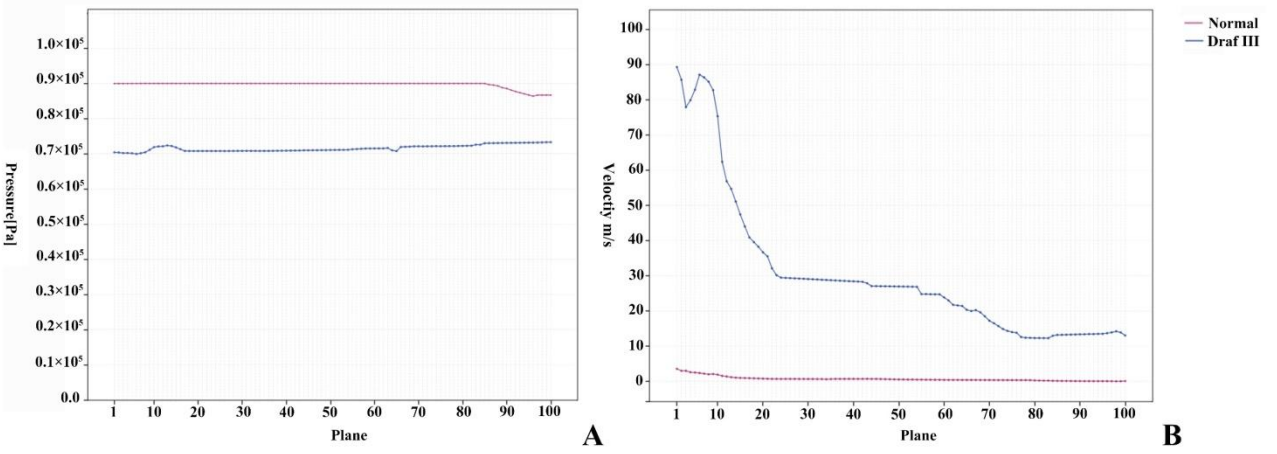

Figure 4. Distribution diagrams of quantitative indexes of airflow of frontal sinus. A: Pressure distribution; B: Velocity distribution. As x-coordinate scale increases, the distance from frontal sinus ostium increased.

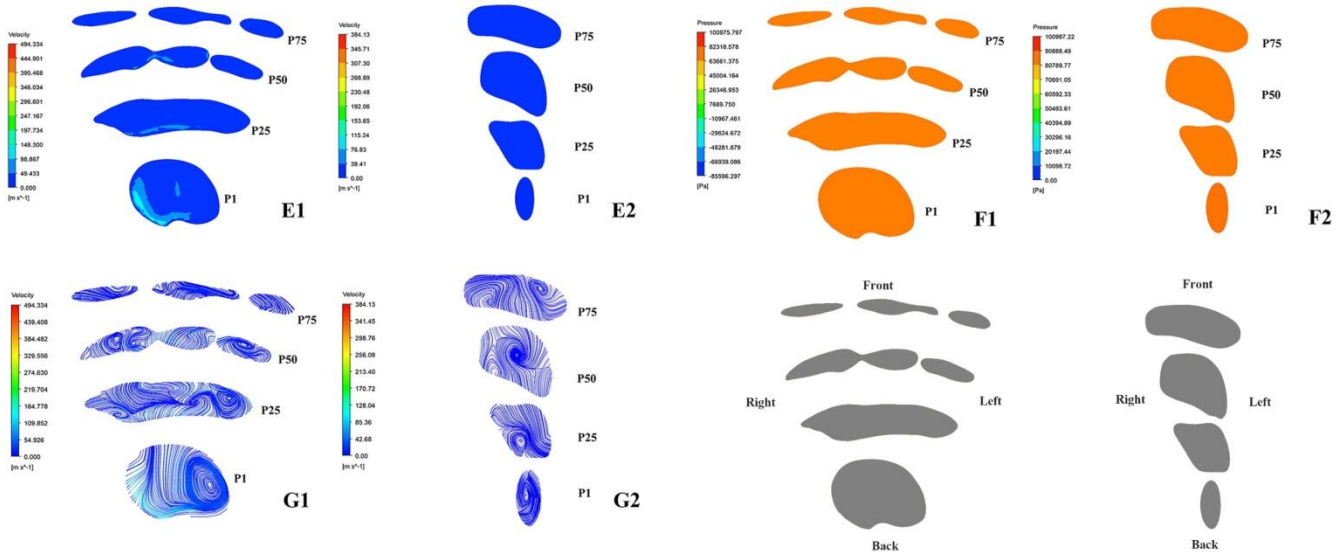

Figure 5. Airflow characteristic patterns in different planes intra-frontal sinus. E1/E2: Velocity field of Draf III/normal model (global pattern). F1/F2: Pressure field of frontal sinus of Draf III/normal model (global pattern). G1/G2: Streamline of frontal sinus of Draf III/normal model (global pattern).

3.3. Airflow pattern of Draf III and normal model

Streamlines (Figure 6) were used to represent airflow patterns. In normal model (Figure 6-R1), airflow pattern in nasal cavity is almost the laminar flow. One turbulence vortex can be found in dorsal region of the nose, with no air flow into the frontal sinus. Airflow pattern of Draf III (Figure 6-R2) in the nasal cavity is similar to that of normal model. However, a larger amount of air can be found flow into the frontal sinus in Draf III model. Flow path showed in Figure 6-R3 by

simulating a small account of air input from the inlet.

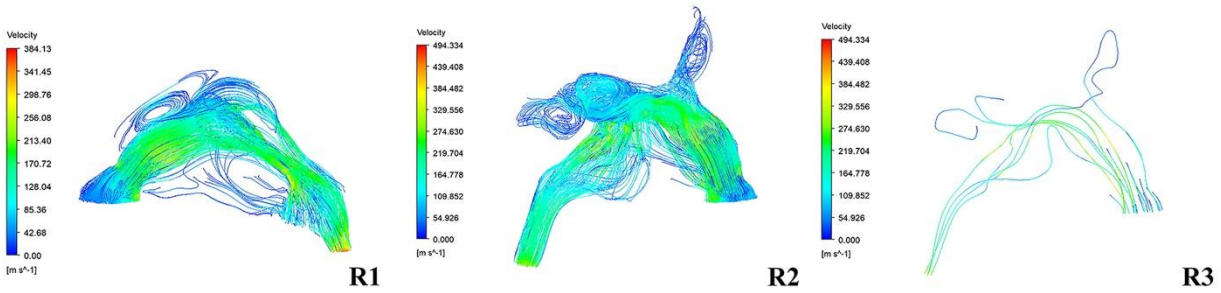

Figure 6. Streamline diagram of normal and Draf III model. R1: Streamline of normal model (Left View). R2: Streamline of Draf III model (Right View). R: Streamline of Draf III model by simulating a small account of air input from the inlet (Right View).

3.4. Comparison of endoscopic appearance and air characteristics

After comparing endoscopic pictures of different postoperative periods after Draf III procedure, edema was found prone to appear at posterior right side in short crus of "Frontal T" structure (Figures 7-A, B and C), which happened to correspond to relatively high-pressure area (Figure 7D).

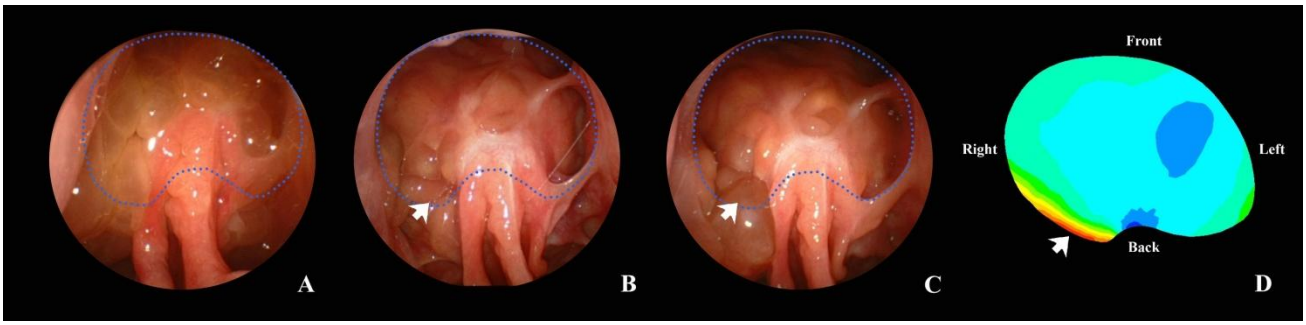

Figure 7. Endoscopic finding of Draf III during postoperative follow-up. A/B/C: Endoscopy at 6 months after surgery/9 months after surgery with methylprednisolone management in last 7 days/12 months after surgery. D: Pressure field of plane in "Frontal T" structure. Blue area represented frontal sinus drainage plane in A, B and C. Edema (B and C) and maximum pressure area (D) was consistent (→).

4. Discussion

Previous studies have shown that normal nasal airflow through the nasal cavity is mainly laminar flow, depending on the individual nasal anatomic form. Sometimes the airflow changes from laminar to turbulent flow in the olfactory region and anterodorsal nasal cavity [17–19]. A similar airflow pattern was seen in the streamline diagram (Figure 6-R1) in normal model of this study. Airflow characteristics of maxillary sinus were extensively studied [20–22]. However, no reports have been published to describe airflow characteristics of frontal sinus.

In this study, relatively high-pressure areas in nasal cavity and sinus mainly appeared at the posterior wall of the frontal sinus ostium (Figures 2-D1, D2). Mean airflow pressure of frontal sinus after Draf III procedure was about 19.3% lower than that of normal subject. Relative differential pressure in the ostium of frontal sinus after Draf III was significantly higher than that of normal subject. After comparison, the intra-frontal sinus airflow pressure after Draf III procedure was significantly lower than normal subject, with an opposite relationship showed in airflow velocity. The quantitative distribution diagram (Figure 4) and cloud map (Figures 5-F1, F2) suggested that absolute value of airflow characters was significantly different, but distribution trends in different sections of airflow characters in frontal sinus were basically the same. Pressure evenly distributed in frontal sinus. Due to the reduction of air resistance after radical removal, airflow velocity at frontal sinus ostium was significantly (10×) higher than that of normal subject. Local relatively high-velocity area could be found in cloud map (Figure 5-E1). Lindemann et al. [23] showed that as flow velocity increased, the absolute temperature gradually decreases in the central area. Therefore, it is theoretically possible that temperature of airflow in frontal sinus after Draf III procedure is likely to be lower than in a normal person. And the authors noted that in laminar flow mode, only airflow close to the mucosa allows for temperature exchange. If a turbulent vortex is formed, the duration of airflow and mucosa contact became longer. From this viewpoint, the formation of vortexes in the frontal sinus after Draf III procedure is more conducive to long-term contact between airflow and mucosa, which contributed to the warming and humidification of inflow air. The effect of this phenomenon on airflow warming and humidification after Draf III procedure requires further research and verification.

In 2005, Lindemann et al. [24] discovered much disorder airflows formed after radical endoscopic removal of the lateral wall of the nasal cavity. However, our study suggests that the intranasal airflow pattern after Draf III procedure is similar to a normal person. Most airflow in normal human model directly entered the nasopharynx through nasal cavity and rarely directly entered the frontal sinus. After Draf III procedure, however, a large amount of airflow went through nasal cavity into the frontal sinus (Figure 6-R2). Inside frontal sinus, pressure and velocity of flow between Draf III and normal models were statistically significant differences ($p < 0.01$) after analyzed by Mann-Whitney U test. Lower pressure, higher velocity and change amplitude of velocity were shown in Draf III model than those in normal subject (Figure 4). However, the airflow patterns in different sections of frontal sinus had similar characteristics between the two models, which was single isolated airflow vortex formed in the frontal sinus ostium (Figures 2-C1, C2) and one or more vortexes formed in frontal sinus (Figures 5-G1, G2). This indicates that the Draf III procedure has little effect on airflow pattern. Variations in airflow patterns are likely to be depending on the resection extent and location. Although Draf III procedure was be considered radical, it can achieve physiological nasal airflow patterns similar to those of normal person. With different values of pressure and velocity compared with normal person, the patients received Draf III procedure still could have no subjective discomfort as shown in this study. The results of this study were based on idealized model of patient with no subjective discomfort, and no abnormality in local mucosa as well as CT scan after strict inclusion criteria. The characteristics differences of airflow caused by individual anatomy, disease severity and surgical techniques need further studies.

Abouali et al. [25] studied the deposition of particulate matter after opening of the maxillary sinus and found that high-velocity airflow can directly enter the opened maxillary sinus. With airflow working as a carrier of microparticles and nanoparticles, deposition of pollutants and drug particles

in the sinus increased. Our collaborative team found that deposition of particulate matter in respiratory tract occurs mainly at locations where the geometry changes dramatically or the airway direction changes. And if there existed higher flow velocity, the more likely deposition will occur [26]. Therefore, a large amount of high-velocity airflow enters the frontal sinus after Draf III procedure will facilitate the transportation and local deposition of nasal spray drug particles. While it also may cause postoperative discomfort due to the deposition of harmful particles such as contaminants and pollen grains.

When flowing through the frontal sinus, the airflow of Draf III model first collided with the right posterior wall of frontal sinus in this model. This position has the following three features: relatively high-pressure area (Figure 2-D1), position of high wall shear stress (Figure 3n), and parts of the airway geometry changed greatly when airflow enters the frontal sinus through nasal cavity. This position exactly corresponds to the right side of short crus of the "Frontal T" in clinical anatomy. In 2006, Draf et al. [16] first proposed the "Frontal T" as a T-shaped structure with the junction between the posterior wall of the frontal sinus (short crus) and forefront of the ethmoid horizontal plate through the nasal septum (long crus), which serves as the safe posterior boundary in establishing the midline drainage channel in Draf III frontal sinus surgery and is also the anatomical mark of frontal sinus. Thus, when positioning the frontal sinus drainage plane, selection of the long and short crus junction of the Frontal T structure that is parallel to the x-y plane is more reasonable than selection of the plane from the frontal nasal crest to the anterior skull base [7]. The real Draf III model was a patient with refractory sinusitis combined with asthma. This patient suffered from asthma attacks 6 months postoperatively accompanied by a large area of edema in the "Frontal T" (Figure 7A). After required oral methylprednisolone for 7 days, the edema significantly improved. However, a small number of vesicles remained on the right side of the "Frontal T" (Figure 7B). After 3 months, isolated large vesicles were seen on the right side of the "Frontal T" under endoscopy (Figure 7C). After eliminating individual factors by self-control comparison, we attributed this tendency to the high shear stress and pressure of airflow on the local mucosa in "Frontal T". Direction and acting effect of wall shear stress are similar to the frictional force. The pressure can be regarded as the result of many gas molecules constantly striking the wall. Therefore, high impact and friction of airflow on the right side of the "Frontal T" may be one reason for postoperative edema. Additionally, changes in the airway direction at this position may lead to deposition of harmful particles that cause edema.

5. Conclusion

This study explored the airflow characteristics in frontal sinus after Draf III procedure. Draf III sinus surgery is able to achieve nasal airflow patterns similar to those of normal person. Although values of airflow pressure and velocity were different from normal person, the patients could have no subjective discomfort after surgery. "Frontal T" structure is a key anatomical site interacted with airflow to be an important cause of postoperative edema after Draf III procedure.

Limitation

The models in this study were simulated by one standard atmosphere, equivalent to the pressure generated by deep breaths. Lack of analysis based on individual anatomical structure and different

surgical techniques and effects of airflow temperature changes are limitations of this study. Future study should increase the sample size, improve the parameters, and explore the outcomes caused by individual anatomical differences and surgical techniques. Also, high impact and friction effects of airflow on "Frontal T" and the possible effects of changes in airway direction require further study.

Acknowledgments

This study was supported by Clinical Medicine Development of Special Funding Support in Beijing Tongren Hospital, Capital Medical University (NO. trzdyxzy201702) and National Natural Science Foundation of China (NO. 81770977) and Beijing Municipal Administration of Hospitals' Ascent Plan (DFL20150202).

Conflict of interest

All authors declare no conflicts of interest in this paper.

References

1. P. J. Wormald, Salvage frontal sinus surgery: The endoscopic modified Lothrop procedure, *Laryngoscope,* **2** (2003), 276–283.
2. W. Draf, Endonasal micro-endoscopic frontal sinus surgery: The fulda concept, Operative Techniques in Otolaryngology-Head and Neck Surgery, **2** (1991), 234–240.
3. L. C. Shih, V. S. Patel and G. W. Choby, et al., Evolution of the endoscopic modified Lothrop procedure: A systematic review and meta-analysis, *Laryngoscope,* **2** (2018), 317–326.
4. N. Choudhury, A. Hariri and H. Saleh, Extended applications of the endoscopic modified Lothrop procedure, *J. Laryngol. Otol.,* **9** (2016), 827–832.
5. C. Georgalas, F. Hansen and W. J. Videler, et al., Long terms results of Draf type III (modified endoscopic Lothrop) frontal sinus drainage procedure in 122 patients: A single centre experience, *Rhinology,* **2** (2011), 195–201.
6. J. M. Yip, K. A. Seiberlin and P. J. Wormald, Patient-reported olfactory function following endoscopic sinus surgery with modified endoscopic Lothrop procedure/Draf 3, *Rhinology,* **2** (2011), 217–220.
7. T. Ye, P. H. Hwang and Z. Huang, et al., Frontal ostium neo-osteogenesis and patency after Draf III procedure: A computer-assisted study, *Int. Forum. Allergy Rhinol.,* **9** (2014), 739–744.
8. D. K. Morrissey, A. Bassiouni and A. J. Psaltis, et al., Outcomes of revision endoscopic modified Lothrop procedure, *Int. Forum. Allergy Rhinol.,* **5** (2016), 518–522.
9. C. Li, B. Zhou and Q. Huang, et al., [Prospective study of the impact on nasal function of the Draf Ⅲ frontal sinus surgery], *Chin. J. Otorhinolaryngol. Head Neck Surgery,* **9** (2014), 1–5.
10. R. Jankowski, D. Pigret and F. Decroocq, et al., Comparison of radical (nasalisation) and functional ethmoidectomy in patients with severe sinonasal polyposis. A retrospective study, *Rev. Laryngol. Otol. Rhinol.,* **3** (2006), 131–140.
11. A. Bassiouni and P. J. Wormald, Role of frontal sinus surgery in nasal polyp recurrence, *Laryngoscope,* **1** (2013), 36–41.
12. X. Liu, Z. Gao and H. Xiong, et al., Three-dimensional hemodynamics analysis of the circle of

Willis in the patient-specific nonintegral arterial structures, *Biomech Model Mechan*, **6** (2016), 1439–1456.
13. P. Xu, X. Liu and H. Zhang, et al., Assessment of boundary conditions for CFD simulation in human carotid artery, *Biomech. Model Mechan.*, **6** (2018), 1581–1597.
14. S. Zhao, Z. Gao and H. Zhang, et al., Robust Segmentation of Intima-Media Borders with Different Morphologies and Dynamics During the Cardiac Cycle, *IEEE J. Biomed. Health*, **5** (2018), 1571–1582.
15. B. Zhou, Q. Huang and S. Cui, et al., Impact of airflow communication between nasal cavities on nasal ventilation, *Orl. J. Otorhinolaryngol. Relat. Spec.*, **5** (2013), 301–308.
16. W. Draf and A. Minovi, The "Frontal T" in the refinement of endonasal frontal sinus type III drainage, Operative Techniques in Otolaryngology-Head and Neck Surgery, **2** (2006), 121–125.
17. K. Zhao and J. Jiang, What is normal nasal airflow? A computational study of 22 healthy adults, *Int. Forum. Allergy. Rh.*, **6** (2014), 435–446.
18. K. Keyhani, P. W. Scherer and M. M. Mozell, Numerical simulation of airflow in the human nasal cavity, *J. Biomech. Eng.*, **4** (1995), 429.
19. J. Wen, K. Inthavong and J. Tu, et al., Numerical simulations for detailed airflow dynamics in a human nasal cavity, *Resp. Physiol. Neurobi.*, **2** (2008), 125–135.
20. J. H. Zhu, H. P. Lee and K. M. Lim, et al., Effect of accessory ostia on maxillary sinus ventilation: A computational fluid dynamics (CFD) study, *Resp. Physiol. Neurobi.*, **2** (2012), 91–99.
21. J. H. Zhu, K. M. Lim and K. T. M. Thong, et al., Assessment of airflow ventilation in human nasal cavity and maxillary sinus before and after targeted sinonasal surgery: A numerical case study, *Resp. Physiol. Neurobi.*, (2014), 29–36.
22. A. A. Gungor, The aerodynamics of the sinonasal interface: The nose takes wing-a paradigm shift for our time, *Int. Forum. Allergy. Rh.*, **4** (2013), 299–306.
23. J. Lindemann, T. Keck and K. Wiesmiller, et al., A numerical simulation of intranasal air temperature during inspiration, *Laryngoscope*, **6** (2004), 1037–1041.
24. J. Lindemann, H. Brambs and T. Keck, et al., Numerical simulation of intranasal airflow after radical sinus surgery, *Am. J. Otolaryng.*, **3** (2005), 175–180.
25. O. Abouali, E. Keshavarzian and P. Farhadi Ghalati, et al., Micro and nanoparticle deposition in human nasal passage pre and post virtual maxillary sinus endoscopic surgery, *Resp. Physiol. Neurobi.*, **3** (2012), 335–345.
26. S. Yu, J. Z. Wang and X. Z. Sun, et al., Numerical analysis on deposition of particulate matters in respiratory tract, *J. Med. Biomech.*, **3** (2016), 193–198.

AIMS Press